



## Research Article

# Fabrication and Analysis of the HLM Method of Layered Polymer Bumper with the Fracture Surface Micrographs

**P. V. Narashima Rao,<sup>1</sup> P. Periyasamy,<sup>1</sup> A. Bovas Herbert Bejaxhin ,<sup>2</sup> E. Vetre Selvan,<sup>3</sup> N. Ramanan,<sup>4</sup> N. Vasudevan,<sup>5</sup> R. Elangovan,<sup>6</sup> and Mebratu Tufa <sup>7</sup>**

<sup>1</sup>Department of Mechanical Engineering, St. Peter's Institute of Higher Education and Research, Avadi, Chennai, India

<sup>2</sup>Department of Mechanical Engineering, Saveetha School of Engineering, SIMATS, Thandalam, Chennai, India

<sup>3</sup>Department of Mechanical Engineering, Sri Sairam Engineering College, West Tambaram, Chennai, India

<sup>4</sup>Department of Mechanical Engineering, PSN Engineering College, Tirunelveli, India

<sup>5</sup>Department of Electronics and Communication Engineering, K. Ramakrishnan College of Technology, Samayapuram, Trichy, India

<sup>6</sup>Department of Mechanical Engineering, Mookambigai College of Engineering, Kalamavur, Pudukkottai 622502, Tamil Nadu, India

<sup>7</sup>Department of Mechanical Engineering, Faculty of Manufacturing, Institute of Technology, Hawassa University, Hawassa, Ethiopia

Correspondence should be addressed to Mebratu Tufa; [mebratu.tufa@hu.edu.et](mailto:mebratu.tufa@hu.edu.et)

Received 9 July 2022; Revised 24 August 2022; Accepted 29 August 2022; Published 4 October 2022

Academic Editor: Vijayananth Kavimani

Copyright © 2022 P. V. Narashima Rao et al. This is an open access article distributed under the Creative Commons Attribution License, which permits unrestricted use, distribution, and reproduction in any medium, provided the original work is properly cited.

Bumpers are essential components that shield passenger cars from slow-speed collisions. Automobiles have them mounted on the front and rear ends. It is believed that bumpers would be crucial in avoiding or restricting damage to automobiles. Various composite material combinations are being researched when a car frontal accident occurs in light of the impact requirements. By comparing it to the parent material, the unique hybrid fibre-metal laminate production clarifies problems such as deformation and stress. This research focuses on identifying the hybrid material composed of basalt fibre with aluminium and glass fibre combinations, inducing it with the properties of the existing parent material and fusing it together to form a laminated composite. It also focuses on identifying its specific features and mapping them with those of the existing ones. This project's peculiarity strives to give the best bumper with a range of deformation between 0.017378 m and 0.03114 m for the 38 MPa tensile strength with a maximum stress prediction of  $2.424 \times 10^2$  MPa that shows advantageous in day-to-day operations, and this is done by comparing simulation results.

## 1. Introduction

The world's attention is currently concentrated on rapid breakthroughs in industries such as aerospace, space, automotive, electronics, and defence, as well as infrastructure and power generation. The automotive industry has emerged as a major economic booster for countries all over the world. Automobile manufacturers are attempting to introduce light-weight, fuel-efficient vehicles to the market. As a result, there is ongoing research towards lowering car costs by

adopting light-weight composites that have similar mechanical properties to metal parts used in automobiles. The current research focuses on the usage of aluminium and basalt fibre composites in the manufacture of automotive bumpers. This aluminium basalt fibre composite is expected to absorb lateral or transverse loading caused by accidents or intentionally occurring occurrences. It is inferred that the fibre metal laminate (FML) exhibits greater bonding strength, exhibiting superior properties [1]. It is noted how composite lamination should be performed [2]. It explains

how reinforcement happens in the FML and explains its characteristics [3]. The paper explains the review of different FML conditions [4]. It explains the conceptual and computational approaches of the FML and how it is performed [5]. It explains the analysis and the methodology adopted to analyse the bumper in Ansys software, and it explains the 3-point bending approach to bumper analysis [6]. For a bumper barrier impact, it explains the presence of an equivalent curved-beam element for the analysis of the bumper [7]. It describes how to analyse a bumper's whole frontal crash barrier and half frontal impact barrier. It also explains how to use ANSYS explicit dynamics for crash analysis [8]. It describes the impact analysis on the wind using finite element analysis with Abaqus software and an auto-towing hook with a steel ball at the end. It describes the parameters for designing and analysing an automotive front end, such as material, thickness, shape, and impact conditions of the beam with bumpers [9, 10]. The tribological behaviour of nonferrous-related material composites has been verified by the experimental verification of wear resistance among the Al6063 metal matrix composite by using the single pass ECAPA route [11]. Better particulate dispersion and more bondage levels can be achieved frequently by using the squeeze casting technique [12]. The defects in casting and grain boundary strengthening have been found through SEM and NDT methods of testing [13]. The tensile and flexural characteristics of natural fibre-reinforced polymer composites have been the focus of Ngo et al.'s research [14]. In this investigation, polylactic acid (PLA), polystyrene (PS), and epoxy (EP) were employed as the matrices to manufacture composites by using Kenaf (KE) and palm empty fruit bunch fibre (EFB) with volume fractions,  $V_f$ , of 20, 40, and 60%. Because of the high proportion of fibre, the tensile strength was at least 29 MPa. According to Luis Angel Lara-González et al.'s discussion in [15], the tensile strength was around 22.88 MPa and reached a high of 56.47 MPa. The mixed fibre composite made of basalt and aluminium has a minimum strength of 38 MPa. [16] Even while this method appears to be successful, it ignores important mechanical characteristics such as fracture toughness. Hybrid PFC has much lower fracture toughness than dentine which has been discussed by Manhart et al.

References [17] Kim and Okuno have discussed that dentine is made up of collagen fibres encased in a hydroxyapatite matrix, whereas hybrid PFC is made out of filler particles embedded in a resin matrix. High fracture toughness materials can more effectively withstand crack initiation and spread. As a result, flexural strength and fracture toughness are crucial factors in determining how long a dental material will last. [18, 19] Garoushi et al. and Lassila et al. have conferred that due to their near resemblance to dentine in terms of microstructure and mechanical characteristics, composite resins reinforced with millimeter-scale short glass fibres (SFRC) are currently the most intriguing materials [20]. It has been established that the material's fibre and matrix-related properties can be used to explain the material's improved resistance to crack propagation also known as fracture toughness, and flexural

strength has been identified by St. Georges et al. [21] Lastumäki et al. have discussed that the UDMA cross-linked matrix, which is plasticized to some extent by using the linear PMMA polymer chains, boosts the flexural strength of composite resin.

In this research work, the absence of strength in metal matrix composites can be determined, and it has been replaced with a novel method of composite preparation, especially from the categories of fibre reinforcements. For superior mechanical qualities, basalt fibre/glass fibres were mixed with nonferrous aluminium alloys to create hybrid polymer composites. The combined form of crash test and deformation simulations can be used with the novelty function, and their comparisons are carried out here. Experimental results based on predictions have been taken into account. These elevated values of tensile and flexural strengths have been obtained, which can be useful for the sustainable development of the fibre-oriented composite. In addition, the applications are huge in size for the implementation of light-weight, high-strength materials which can be used for automotive and aircraft body applications. The simulations are held in hands to step up to the next level based on their predicted stresses and deformations, and they can fulfill the future scope.

## 2. Materials and Methods

*2.1. Fabrication of FML with Layers.* The hand lay-up method of composite processing is the most basic. This strategy also has a low infrastructure need. The processing steps are simple to follow. To begin with, a release gel is sprayed on the mould surface to keep the polymer from sticking. Reinforcement in the form of woven mats or chopped strand mats is trimmed to meet the dimensions of the mould and then put on the surface of the mould. The liquid thermo-setting polymer is then thoroughly mixed with a pre-determined hardener (curing agent) and poured onto the surface of the previously prepared mat in the mould as shown in Figure 1. The ASTM D 790 criteria are followed in the preparation of the flexural specimens. The test specimens of each laminate of aluminium basalt fibre reinforced epoxy composites are manufactured and evaluated by using the same UTM to apply the three-point flexural stress. The 3-point flexural test is the most frequent flexural test, and it was employed in this experiment to determine the composite materials' bending strength. Placing the test specimen in the UTM and applying force to it until it fractures and breaks is the testing procedure. The result of the specimen's flexural strength is seen. Table 1 shows the results of the experiments. A hand layup is depicted in Figure 2. The capital and infrastructure needs are reduced as compared to other alternatives. The manufacturing rate of treated composites is reduced, and attaining a large volume fraction of reinforcement is difficult.

*2.2. Tensile Testing.* The characteristics of fibres and their orientation, which determine the quality of the produced composite laminate, are influenced by a variety of factors.

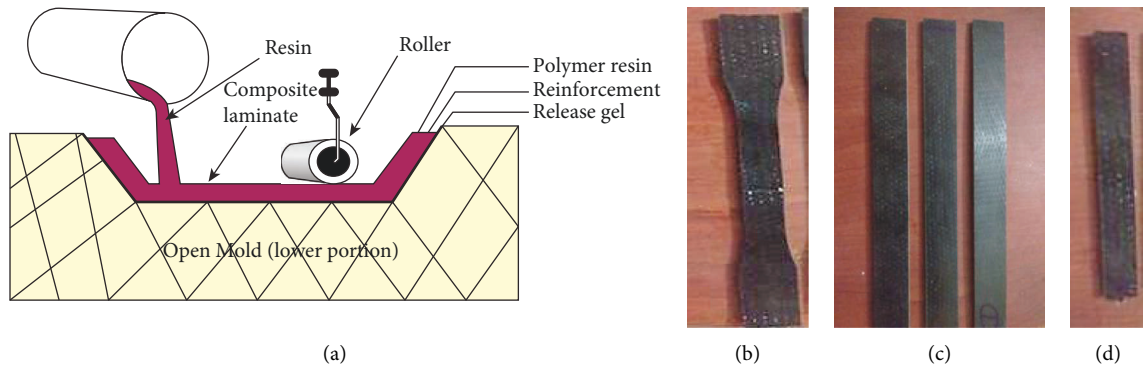


FIGURE 1: (a) Hand lay-up method of fibre metal laminate [22], (b) specimen for tensile testing, (c) samples of the impact test, and (d) sample for the flexural test.

TABLE 1: experimental value for flexural strength.

Specimen	Sample (KN)
Basalt fibre	161
Basalt and aluminium fibre	192
Glass fibre	120
Aramid fibre	192

TABLE 2: experimental value for tensile strength.

Specimen	Tensile load (KN)	Tensile strength (N/mm <sup>2</sup> )
Basalt fibre	3.2	34
Basalt fibre and aluminium fibre	3.6	38
Glass fibre	2.8	22
Aramid fibre	3.8	44

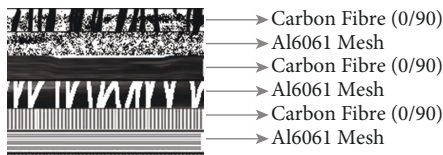


FIGURE 2: FML layers of the laminate.



FIGURE 3: UTM tensile testing of the sample specimen.



FIGURE 4: Flexural testing of the specimen sample.

The impact of fibre parameters is discussed further down. The dimensions of the tensile test specimens are taken into consideration. It is made in accordance with ASTM-D638 methods and standards. The laminate specimen is used to test the tensile behaviour of composite laminates. On the Universal Testing Machine (UTM), as depicted in Figure 3, the tensile test is carried out by applying load to the specimen until it fails, and the results are recorded. The constructed laminate as shown in Figure 3 was put through a tensile test in accordance with ASTM-D638. After the test, the trials provided tensile strength results. Table 2 shows the results of the experiments.

2.3. *Flexural Testing.* Flexural specimens are prepared in accordance with ASTM D 790 standards. Each laminate of aluminium basalt fibre reinforced epoxy composite is fabricated and assessed by using the same UTM to apply the three-point flexural stress. The 3-point flexural test is the most common flexural test, and it was used in this experiment to evaluate the bending strength of the composite materials, as shown in Figure 4. The testing process consists of placing the test specimen in the UTM and exerting force on it until it fractures and breaks. The flexural strength of the specimen is demonstrated, and the outcomes of the trials are shown in Table 1.

2.4. *Impact Testing.* Impact test specimens are constructed to the necessary dimensions in accordance with the ASTM-A370 standard as depicted in Figure5. During the testing procedure, the test specimen is inserted into the UTM. The

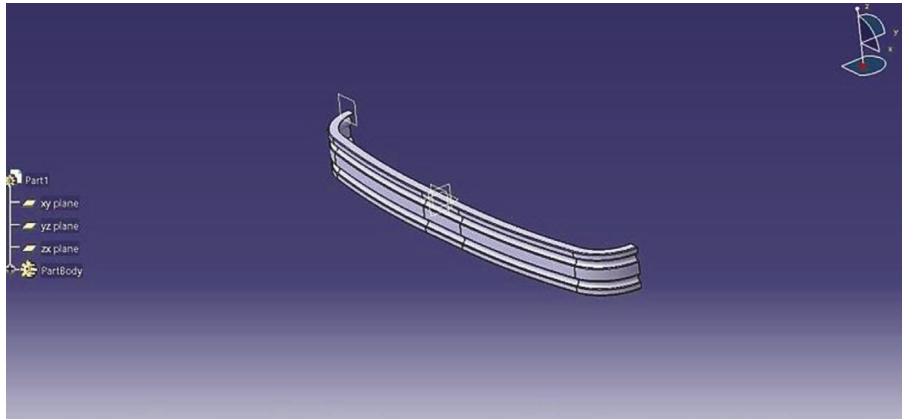


FIGURE 5: CATIA V5 model of the bumper.



FIGURE 6: Impact testing of the sample specimen.

TABLE 3: Experimental values of absorbed energy using the impact test.

Specimen	Absorbed energy (J)
Basalt fibre	7
Basalt and aluminium fibre	8
Glass fibre	7
Aramid fibre	14

specimen must be inserted into the testing apparatus, allowing the pendulum to fracture the specimen as mentioned in Figure 6. The impact test can simply determine the maximum energy necessary to shatter the material. The maximum energy absorbed by the various specimens, particularly aramid fibre, has been determined to be 14 J, as shown in Table 3.

### 3. Design and Analysis of the Modelled Bumper

**3.1. Modelling of the Bumper.** CATIA (computer-assisted three-dimensional interactive application) is a multiplatform computer-aided design (CAD), computer-aided manufacturing (CAM), and computer-aided engineering (CAE) software package developed by Dassault Systemes.

CATIA has unrivalled capabilities for modelling any product in the context of its real-world behaviour: design in the age of experience. System architects, engineers, designers, and all other stakeholders may define, conceive, and shape the linked world. To build 3D CAD models of the aluminium specimen as shown in Figure 5, CATIA V5 is utilized.

The finite element approach is a numerical approximation method in which a complicated structure is broken down into a number of little bits or pieces, which are referred to as finite elements. These microscopic elements are linked together by nodes, which are small points that connect them with the incorporation of a convergence type of mesh generation. The finite element approach is also known as structural analysis because it uses matrix algebra to solve simultaneous equations. It is quickly becoming the major analytical tool for designers and analysts.

**3.2. Stress and Total Deformation.** Total deformation and directional deformation are phrases that are used interchangeably in finite element methods, regardless of the software employed. Directional deformation refers to the movement of the system along a certain axis or in a user-defined direction. The total deformation is the vector sum of all the directional displacements of the systems. Figures 7(a) and 7(b) show a detailed comparison of the deformation levels of the basalt fibre bumper and basalt aluminium fibre under 3-point bending. The complete deformation of the basalt fibre bumper under 3-point bending is shown in Figures 7 and 8.

The comparison between the tensile strength and load for various fibre and composite materials is mentioned in Figure 9. Here, the tensile strength of  $44 \text{ N/mm}^2$  is recorded in aramid fibre under a load condition of 3.6 kN. In comparison, the tensile strength of glass fibre, basalt, and aluminium fibre composites was attained with higher entities. The loads have tensile strengths of 3.6 kN and 3.8 kN, respectively, which have been identified through the peaks obtained in Figure 9. If the load becomes a maximum of 3.5 kN or greater, the basalt fibre and aluminium fibre composites produce higher tensile strength values.

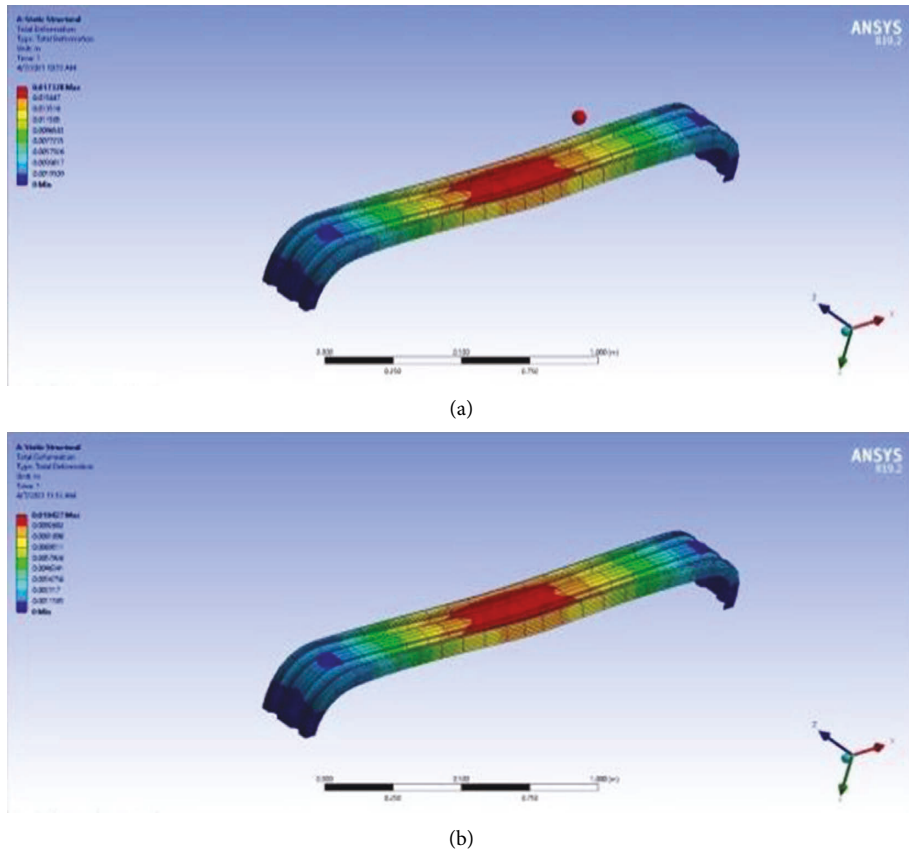


FIGURE 7: Total deformation of (a) basalt fibre bumper and (b) basalt aluminium fibre.

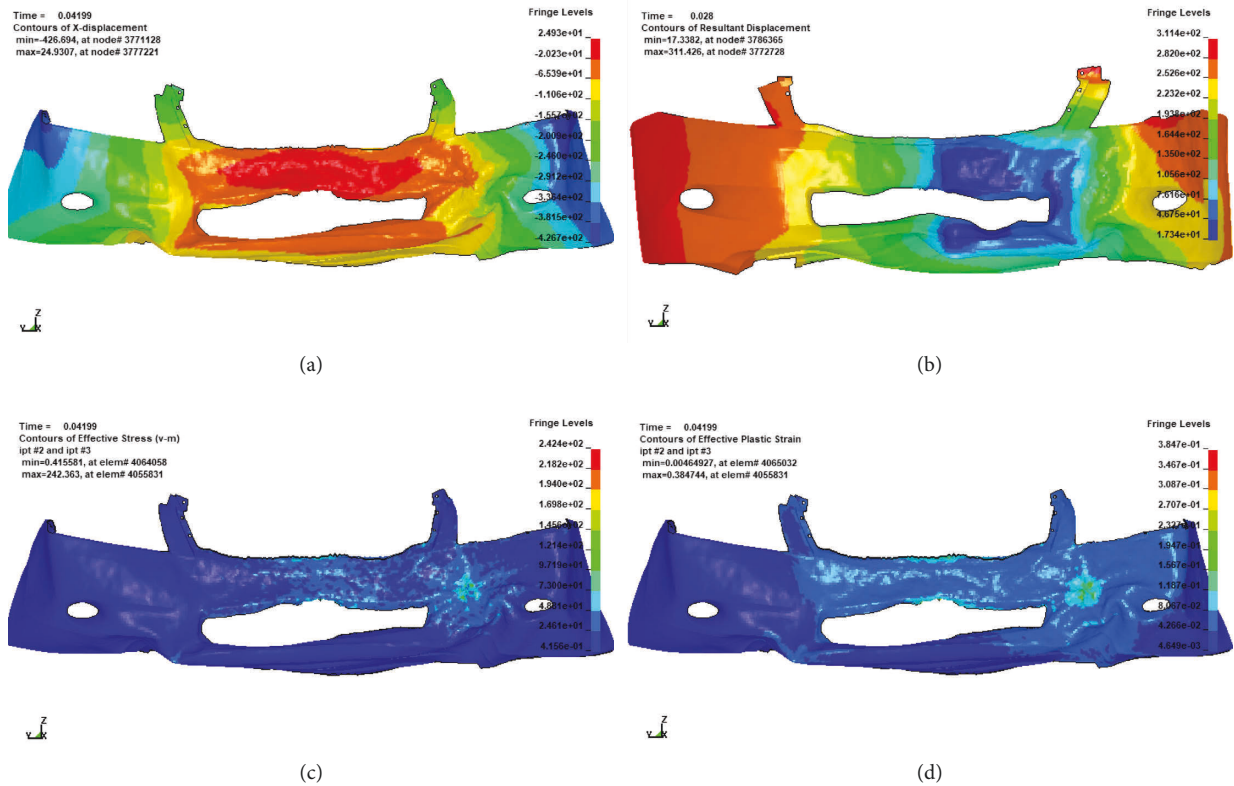


FIGURE 8: Crash test simulation results by using FEA (a) resultant displacement of the frontal crash of basalt fibre (b) resultant displacement of the frontal crash of basalt fibre with aluminium (c) effective von Mises stress (d) effective plastic strain.



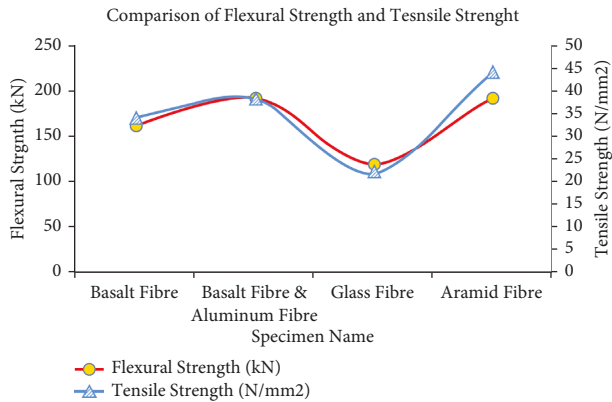


FIGURE 9: Comparison of flexural strength and tensile strength.

The strong bonding of fibre reinforcement can provide an effective bending moment while also withstanding more fluctuations. The material contribution was obtained among the layerwise specimens, which can reveal remarkable strength in both tensile as well as impact testing. Figures 7 and 8 show that the curvature area of the basalt aluminium fibre bumper showed more and less deformation of 0.03114 and 0.017378 m. More concentration of stress was obtained at its centre. A higher stress of  $2.424 \times 10^2$  MPa can be obtained by using the basalt fibre bumper during the frontal crash simulation. [14] Ngo et al. have focused on the tensile and flexural properties of natural fibre reinforced polymer composites. In this study, Kenaf (KE) and palm empty fruit bunch fibre (EFB) with volume fractions of Vf of 20%, 40%, and 60% were used in this study to prepare composites that comprised polylactic acid (PLA), polystyrene (PS), and epoxy (EP) as the matrices. The tensile strength was attained at a minimum of 29 MPa due to the percentage of fibre addition up to 20% according to the discussion of [15] Lara-González et al. The tensile strength was found to be nearly 22.88 MPa, with a maximum of 56.47 MPa. Comparatively, the basalt fibre and aluminium combined fibre composite has attained a 38 MPa as minimum. It can withstand more tensile loads compared with other fibre composites.

A crash test is a type of destructive testing that is frequently carried out to guarantee that crashworthiness and crash compatibility standards are met for various means of transportation, automobile safety, or associated systems and components. The front panel body of the vehicle can be involved in this crash test. The real-time structural damages can be verified through the simulation platform by applying some trail loads for the required boundary conditions. The body dynamics and materials involved in any automotive components based upon the unchanging or nonidentical pressures can be analysed through this software tool.

The impacts of strain rate sensitivity of CFRE, BFRE, and their mixes were investigated, according to Yao et al. [23]. Cross-sections of the cracked specimens were analysed. The findings showed that all of the hybrid composites were sensitive to the stacking order. In the quasistatic condition, the peak forces of two hybrid constructions were between those of basalt fibre reinforced composite and carbon fibre

reinforced composite, with H1 and H2 improved by 3 MPa and 29 MPa, respectively, compared to BFRE. [24] According to Zuzana Marcalikova et al., the augmentation of fibre content in the composite construction boosted tensile strength. [25] Tensile tests revealed that laminates with modified F584-epoxy matrix had better mechanical characteristics than laminates with F155-epoxy matrix. The F584/PW family has the greatest tensile strength, while the F584/8HS family has the highest modulus.

The frontal crash of the polymer bumper has been identified with the simulation outcomes such as deformation and von Mises stress. The resultant displacement of the front crash of the bumper shown in Figure 8(a) indicates that more deformation  $2.493 \times 10^{-2}$  mm has occurred at the exact centre region of the basalt fibre composite front bumper. Similarly, as shown in Figure 8(b), a reasonable deformation of  $3.114 \times 10^{-2}$  mm has been identified for the aluminium-combined basalt fibre bumper. In addition to that, the effective von Mises stress and strain were obtained for the applied load, which can be considered for the fixed boundary conditions. Because of the safe load and its extreme level, this design fails. Utilizing CATIA V5 simulation studies, the composite bumper solid model with the simply supported type was developed utilizing the parameters for determining the safe design and loading. Since both ends are fixed, there is zero displacement. In this research investigation, the static mode of analysis was used.

Load: 3 KN to 5 KN (based on tensile, impact, and flexural strength)

Model: composite bumper solid model (CATIA-V5)

Type of model: simply supported

Boundary conditions: both the ends of the bumper as the fixed position for static and front crash test (zero displacement at the fixed ends)

Figure 10 depicts the relationship of tensile strength to tensile load for the basalt fibre, basalt fibre and aluminium fibre composite, glass fibre, and aramid fibre. The triangular yellow marker represents the range of tensile strength, which has been connected with the curved red lines. The bar represented the value of the tensile load acting on the specimen while conducting the test. Tensile properties vary depending on the closeness of the polymer structure in the specimen. Basalt and glass fibre, in particular, were recognized as having no previous reinforcements. However, in aramid and basalt-aluminium fibres, the impact of homogeneous reinforcements is combined. This might be demonstrated by the excellent tensile results indicated in Figure 11 microstructures.

Due to the changes in material composition or composite matrix, nearly identical ranges of flexural and tensile strength have been attained. Probably, the basalt fibre and aluminium combined form of the specimen have attained a secondary level of better outcomes in tensile strength. The aramid fibre was observed as a robust material composite which will be used for more applications. On the other hand, comparative analyses have been carried out over the same materials for the parameters of flexural strength and tensile

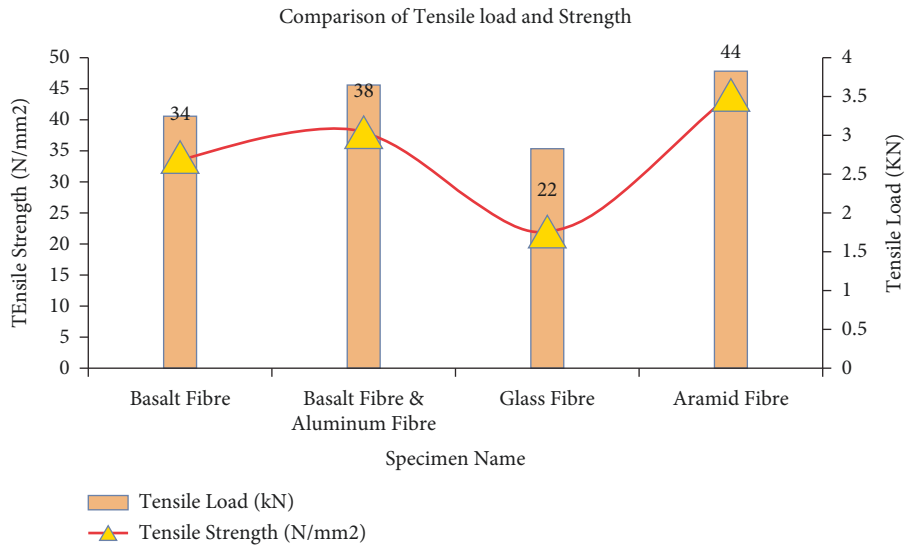


FIGURE 10: Comparison of tensile strength for different tensile loads.

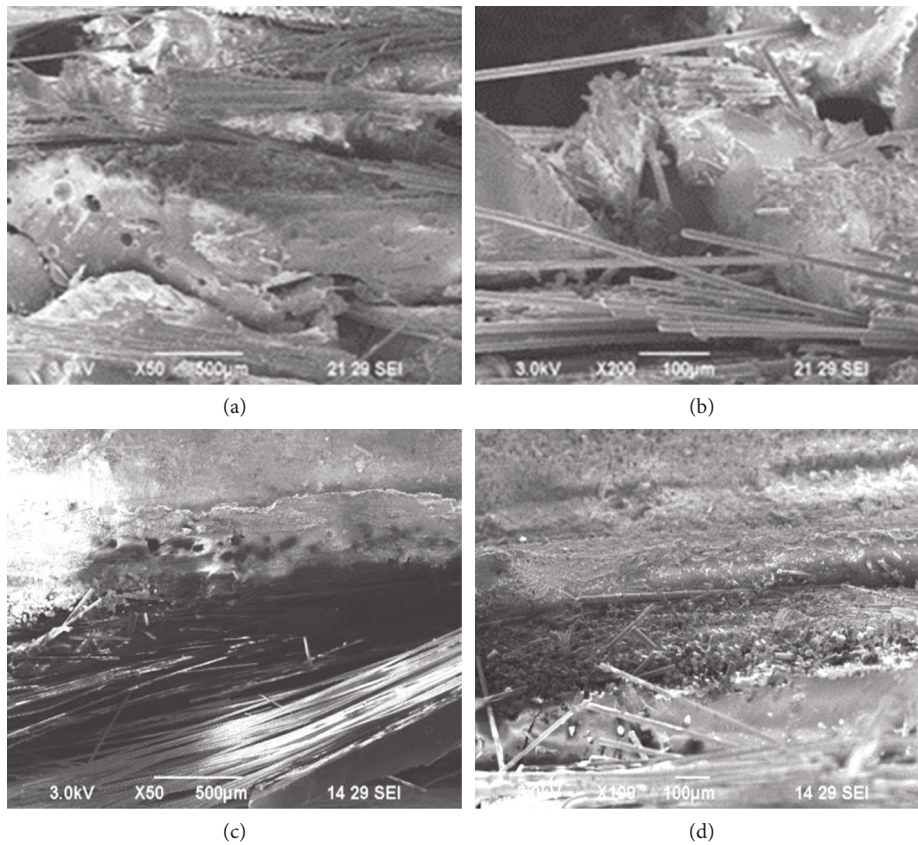


FIGURE 11: SEM images of fractures and surfaces of the FLM layer composite of (a) basalt fibre, (b) basalt-aluminium fibre, (c) glass fibre, and (d) aramid fibre.

strength. The blue smooth line curve represents the tensile strength, and the red-lined yellow bullets depict the flexural strength. Figure 9 depicts the intermittent coincident between tensile and flexural strength.

The exact same coincidence happened for the basal fibre and aluminium fibre, which shows that it can withstand higher load applications with acceptable flexural and equivalent tensile strength. The same conditions are suitable

which have been obtained for the aramid fibre with elevated tensile properties.

#### 4. Microstructural Evidence of Fracture Surface Images

The topography of the surface is determined by the interaction between the tool and the properties of the material being machined. Mechanical testing showed that during the extruded profile, the tested material's mechanical properties changed. Microscopical analysis of the material's structure revealed the heterogeneity of the composite and the presence of small fractures where the wood particles and polymer matrix contacted one another. SEM creates image samples that are used to examine the specimen's topography and morphology. It depicts the cracked surfaces of test specimens that are examined by using a scanning electron microscope (SEM). The relationship between the tool and the quality of the machined material determines the topography of the surface. Mechanical tests demonstrated that the material's mechanical characteristics change throughout the extruded profile. The composite's heterogeneity was revealed by microscopic examination of the material's structure, which also revealed the presence of tiny fissures at the points where the wood particles and polymer matrix came into contact.

The damage caused by the specimen's tensile test is depicted in Figure 11. Various magnification levels have been maintained for taking these observations as 50X, 100X, and 200X with a size factor of 100  $\mu\text{m}$  and 500  $\mu\text{m}$ , respectively. Simple basalt fibre having major white spots indicated as a pure form of basalt fibre. Figure 11(b) clearly shows that fibre breakage occurs in basalt-aluminium fibre as a result of a sheer action that is not uniform across the surface due to the presence of twisted fibres that oppose each other in the opposite direction, eventually achieving stability. Figure 11(c) shows that the distribution of brittle-rich glass particles is clearly indicated by the dark and closely spaced lines structure. Figure 11(d) depicts the particle distribution of aramid fibres by using solid coloured even surfaces. A scanning electron microscope was used to create the images. A ductile fracture is depicted in this illustration. Porosity is caused by the generation of exothermal heat.

#### 5. Conclusion

Automobile manufacturers are attempting to introduce light-weight, fuel-efficient vehicles to the market. As a result, there is ongoing research towards lowering car costs by adopting light-weight composites that have similar mechanical properties to metal parts used in automobiles. The following conclusions have been made:

- (i) The current research focuses on the usage of aluminium and basalt fibre composites in the manufacture of automotive bumpers. This aluminium glass fibre composite is expected to absorb lateral or transverse loading caused by accidents or intentionally occurring occurrences.

- (ii) The performance of composite materials is examined using a three-point bending technique in this study. It is a type of internal mode failure caused by fibre layer separation in a composite laminate. The delaminated specimen with its voids and blowholes is shown in the illustration. It has also been discovered that during the separation of layers, the medium's adhesion is not greatly changed, resulting in less damage to the laminate.
- (iii) The specimen was subjected to a two-fold shear test, which resulted in this damage. Because of the twisted fibres resisting each other in the opposite direction, the shear effect causes fibre breakage that is not uniform over the surface, so it achieves a stable condition.
- (iv) In CATIA V5, the proposed fibre metal laminate of basalt and aluminium was conceived as a bumper. The design was loaded into ANSYS APDL software, and a three-point bending technique was used on both the basalt fibre bumper and the basalt-aluminium fibre bumper. Equivalent stress and deformation values were obtained and compared.

#### Data Availability

The data used to support the findings of this study are included within the article. Should further data or information be required, these are available from the corresponding author upon request.

#### Disclosure

It was performed as a part of the Employment Hawassa University, Ethiopia.

#### Conflicts of Interest

The authors declare that they have no conflicts of interest.

#### Acknowledgments

The authors would like to thank the Saveetha School of Engineering, SIMATS, Chennai 602 105, Tamil Nadu, India, for their excellent support for the submission of their papers.

#### References

- [1] E. A. TamerSinmazçelik and M. ÖzgürBora, "OnurÇoban A Review: Fibre Metal Laminates," *Background, Bonding Types and Applied Test Methods*, vol. 32, 2011.
- [2] K. Kavitha, R. Vijayan, and T. Sathishkumar, "Fibre-metal laminates," *A review of reinforcement and formability characteristics*, vol. 22, 2020.
- [3] R. Khan, "Fiber Bridging in Composite Laminates," *A Literature Review*, vol. 229, 2019.
- [4] M. Chandrasekar, M. R. Ishak, M. Jawaid, Z. Leman, and S. M. Sapuan, "An Experimental Review on the Mechanical Properties and Hygrothermal Behaviour of Fibre Metal Laminates," *Journal of Reinforced Plastics and Composites*, vol. 36, 2016.



- [5] Kreja Ireneusz, "A Literature Review on Computational Models for Laminated Composite and sandwich Panels," *Open Engineering*, vol. 25, 2011.
- [6] P. B. Biradar and Kajol Kamat, "Dharmadeep Sarkate, Sagar Jamdade, Design and analysis of Bumper," vol. 34, 2018.
- [7] D.-K. Park, "Bumper Impact Using the Dynamically Equivalent Beam Approach," *International Journal of Automotive Technology*, vol. 25, 2011.
- [8] M. Karthikeyan, M. P. Jenarathanan, R. Giridharan, and K. Shunmugesh, "Investigation on Crash Analysis of a Frontal Car Bumper," *Transactions of the Indian Institute of Metals*, vol. 12, 2011.
- [9] A. Calieniug and N. Radu, "Design and FEA Crash Simulation for a Composite Car Bumper," *Engineering Sciences*, vol. 5, 2012.
- [10] J. Marzbanrad and M. Alijanpour, "Mahdi Saeid Kiasat Design and Analysis of an Automotive Bumper Beam in Low-Speed Frontal Crashes," *Elsiver*, vol. 47, 2009.
- [11] P. Sureshkumar, T. Jagadeesha, L. Natrayan, M. Ravichadran, D. Veeman, and S. M. Muthu, "Electrochemical corrosion and tribological behaviour of AA6063/Si<sub>3</sub>N<sub>4</sub>/Cu (NO<sub>3</sub>)<sub>2</sub> Composite processed using single-pass ECAPA route with 120° die angle," *Journal of Materials Research and Technology*, vol. 16, pp. 715–733, 2022.
- [12] L. Natrayan and M. Senthil Kumar, "A novel feeding technique in squeeze casting to improve reinforcement mixing ratio," *Materials Today Proceedings*, vol. 46, pp. 1335–1340, 2021.
- [13] A. Bovas Herbert Bejaxhin, G. Paulraj, and M. Prabhakar, "Inspection of casting defects and grain boundary strengthening on stressed Al6061 specimen by NDT method and SEM micrographs" *Journal of Materials, Research and Technology*, vol. 8, no. 3, pp. 2674–2684, 2019.
- [14] W. L. Ngo, M. Pang, L. Yong, and K. Y. Tshai, "Mechanical properties of natural fibre (Kenaf, oil palm empty fruit bunch) reinforced polymer composites," *Advances in Environmental Biology*, vol. 8, pp. 2742–2747, 2014.
- [15] L. Á. Lara-González, W. Guillermo-Rodríguez, Y. Pineda-Triana, G. Peña-Rodríguez, and H. F. Salazar, "Optimization of the tensile properties of polymeric matrix composites reinforced with magnetite particles by experimental design," *TecnoLógicas*, Mayo-Agosto, vol. 23, no. 48, 2020.
- [16] J. Manhart, K. H. Kunzelmann, H. Y. Chen, and R. Hickel, "Mechanical properties and wear behavior of light-cured packable composite resins," *Dental Materials*, vol. 16, pp. 33–40, 2000.
- [17] K. H. Kim and O. Okuno, "Microfracture behaviour of composite resins containing irregular-shaped fillers," *Journal of Oral Rehabilitation*, vol. 29, pp. 1153–1159, 2002.
- [18] S. Garoushi, P. K. Vallittu, and L. V. J. Lassila, "Short glass fiber reinforced restorative composite resin with semi-interpenetrating polymer network matrix," *Dental Materials*, vol. 23, pp. 1356–1362.
- [19] L. Lassila, S. Garoushi, P. K. Vallittu, and E. Säilynoja, "Mechanical properties of fiber reinforced restorative composite with two distinguished fiber length distribution," *Journal of the Mechanical Behavior of Biomedical Materials*, vol. 60, pp. 331–338, 2016.
- [20] A. J. Georges, E. J. Swift, J. Y. Thompson, and H. O. Heymann, "Irradiance effects on the mechanical properties of universal hybrid and flowable hybrid resin composites," *Dental Materials*, vol. 19, pp. 406–413.
- [21] T. M. Lastumäki, L. V. Lassila, and P. K. Vallittu, "The semi-interpenetrating polymer network matrix offiber-reinforced composite and its effect on the surface adhesive properties," *Journal of Materials Science: Materials in Medicine*, vol. 14, pp. 803–809, 2003.
- [22] <https://www.eppcomposites.com/hand-layup-process.html>.
- [23] Y. Yao, J. Cui, S. Wang et al., "Comparison of tensile properties of Carbon fiber, basalt fiber and hybrid fiber reinforced composites under various strain rates," *Applied Composite Materials*, vol. 29, 2022.
- [24] Z. Marcalikova, M. Racek, P. Mateckova, and R. Cajka, "Comparison of tensile strength fiber reinforced concrete with different types of fibers," *Procedia Structural Integrity*, vol. 28, pp. 950–956, 2020.
- [25] Jane Maria Faulstich de Paiva, S. . Mayer, and M. Cerqueira Rezende, "Comparison of tensile strength of different Carbon fabric reinforced epoxy composites," *Materials Research*, vol. 9, no. No. 1, pp. 83–89, 2006.
- [26] M. Nasiruddin, A. Hambali, J. Rosidah, W. S. Widodo, and M. N. Ahmad, "A review of energy absorption of automotive bumper beam," *International Journal of Applied Engineering Research*, vol. 12, no. 2, p. 12, 2017.
- [27] P. Kumar Uddandapu, "Impact Analysis on Car Bumper by Varying Speeds Using Materials ABS Plastic and Poly Ether Imide by Finite Element Analysis Software Solid Works," *International Journal of Modern Engineering Research (IJMER)*, vol. 3, 2013.